

Mechanical properties of the iron-based superconductor $\text{SmFeAsO}_{1-x}\text{F}_x$

W Malaeb¹, I Kazah¹, R Awad¹ and M Fujioka²

¹Physics Department, Faculty of Science, Beirut Arab University, Beirut 11-5020, Lebanon

²Research Institute for Electronic Science, Hokkaido University, Sapporo, Hokkaido 001-0020, Japan

Email: w.malaeb@bau.edu.lb

Abstract. We have investigated the mechanical properties of the iron-based superconductor (FeSC) $\text{SmFeAsO}_{1-x}\text{F}_x$ (Sm1111) with a wide doping range $0.09 \leq x \leq 0.3$ by performing the Vickers microhardness test. The estimated Vickers microhardness number (H_v) was analysed using Meyer's law, Hays-Kendall approach, elastic/plastic deformation (EPD) model and proportional specimen resistance (PSR) model, where the PSR model showed the best match with our experimental data. H_v values showed an increase as x increases, indicating that fluorine doping results in an improvement in the mechanical properties of the Sm1111 compound and makes it more convenient for applications.

1. Introduction

There has been much interest in iron-based superconductors (FeSCs) [1] which have been extensively studied recently [2-5]. $\text{SmFeAsO}_{1-x}\text{F}_x$ (Sm1111) belongs to what is known as the "1111" FeSC family, and still keeps the highest bulk T_c record of around 58 K [6, 7]. It was reported that with F doping in Sm1111, the crystallographic transition from the tetragonal to the orthorhombic structure disappears and superconductivity (SC) simultaneously appears at $x \approx 0.06-0.08$ and T_c^{onset} rapidly increases above $x=0.08$ [6]. Also XRD data show that the impurity phases start to increase from $x=0.16$ [6]. Given the high T_c value in addition to its large upper critical field and high magnetic critical current density reaching $1.5-2 \times 10^4 \text{ A/cm}^2$ [8], Sm1111 has been considered a promising candidate for applications such as wires and tapes [6]. For this reason, many of its properties have been studied [6, 7], yet some other properties have not been fully studied like the mechanical properties which are very critical to judge the convenience of a compound for applications. An important mechanical property is the microhardness, the measure of the material's resistance to localized plastic deformation like small dents or scratches [9]. A popular microhardness measuring technique is the Vickers indentation method [9] which we have implemented here to determine the Vickers microhardness number (H_v) of a wide doping range $0.09 \leq x \leq 0.3$ of Sm1111. H_v results showed a normal indentation size effect (ISE) similar to several cuprate systems [10-13]. In addition, H_v values showed an increase as x increases indicating that fluorine doping results in an improvement in the mechanical properties of the Sm1111 compound and makes it more convenient for applications.

2. Experimental technique

The Vickers microhardness measurements of Sm1111 samples with $0.09 \leq x \leq 0.3$ were carried out in atmospheric air at room temperature using a digital microhardness tester (MHVD-1000IS). The loads



applied on the sample surface by the pyramidal indenter varied between 0.49 and 9.8 N with different loading times varying between 10 and 60 s in steps of 10 s. To guarantee the surface position independence of the collected data, the indentations were made at three different regions of the surface from which an average H_v value was evaluated for each load. The Vickers microhardness number H_v is defined as the ratio of the applied load to the pyramidal contact area of indentation, and is given as:

$$H_v = 1854.4 \frac{F}{d^2}, \quad (1)$$

where F is the applied load in Newton and d is the diagonal length in micrometers.

3. Results and discussion

The variation of the Vickers microhardness number H_v calculated from equation (1), with the applied load F for Sm1111 samples with $0.09 \leq x \leq 0.3$ is displayed in figure 1. The first observation is that for all doping levels, H_v decreases as F increases reaching saturation at high loads. This behavior, known as the indentation size effect (ISE), has been observed in several cuprate systems [10-13]. However, it is sharper in cuprates compared to what is observed here for the FeSCs case which probably indicates better grain connectivity in FeSCs compared to cuprates. Second, we notice that H_v increases as the doping content x increases up to $x=0.22$ beyond which no considerable increase is observed. Similar to the case of cuprates, the increase of H_v values as x increases may be attributed to the reduction of porosity, the resistance to crack propagation among the grains and the increase of grain connectivity [10-13] resulting from replacing oxygen with fluorine. Therefore, a general trend of the effect of fluorine doping in Sm1111 compound is an improvement in the mechanical properties which makes it more convenient for applications.

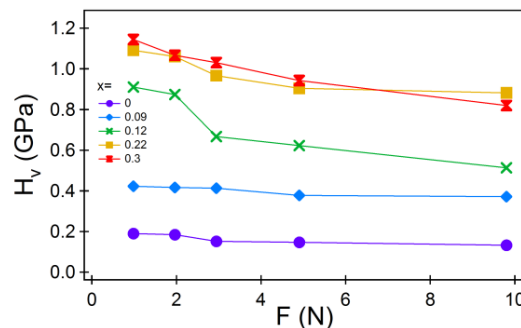


Figure 1. Variation of H_v with F at a dwell time of 40 s for $\text{SmFeAsO}_{1-x}\text{F}_x$ with $x=0, 0.09, 0.12, 0.22$ and 0.3 .

Next we present in figure 2 our data analysis according to Meyer's law [14], Hays and Kendall (HK) approach [15], the elastic/plastic deformation (EPD) model [16, 17] and the proportional specimen resistance (PSR) model [10-13]. To check Meyer's law given by equation (2), $\ln F$ is plotted as a function of $\ln d$ in figure 2 (a). For all doping levels, the exponent n known as the Meyer number is less than 2 which indicates a normal ISE in agreement with other high- T_c superconductors like cuprates [10-13] and MgB_2 compound [18].

$$F = Ad^n \quad (2)$$

The values of W_{HK} , the limiting applied force value and the load-independent microhardness constant A_1 according to the HK model given by Eq. (3) were determined from F vs. d^2 plot displayed in figure 2 (b) and the obtained values are listed in table 1.

$$F - W_{HK} = A_1 d^2 \quad (3)$$

HK load-independent microhardness values (H_{HK}), listed in table 1, were obtained from Eq. (4):

$$H_{HK} = 1854.4 \frac{F - W_{HK}}{d^2} \quad (4)$$

The constants A_2 and d_0 values, related to the EPD model expressed by equation (5), were determined from figure 2 (c) where $F^{0.5}$ is plotted versus d and listed in table 1.

$$F = A_2(d + d_0)^2 \quad (5)$$

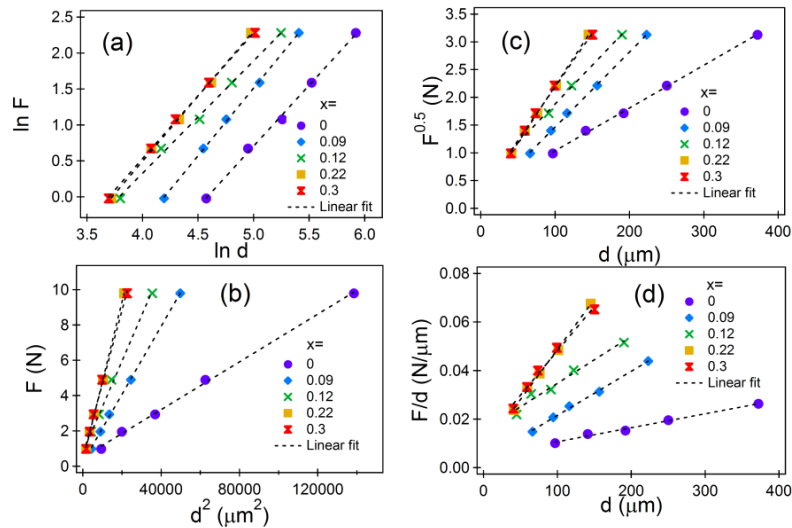


Figure 2. Vicker's microhardness data of $\text{SmFeAsO}_{1-x}\text{F}_x$ with $x=0, 0.09, 0.12, 0.22$ and 0.3 analyzed according to (a) Meyer's law: variation of $\ln(F)$ with $\ln(d)$, (b) HK approach: variation of the applied force (F) with the square of the semi-diagonal length (d), (c) EPD model: variation of $(F^{0.5})$ with (d), and (d) PSR model: the ratio (F/d) versus (d). In each plot, the dotted lines represent the linear fitting of the data corresponding to each doping level from which the fitting parameters of table 1 were determined (refer to text).

Then the elastic/plastic deformation load-independent microhardness H_{EPD} is evaluated from Eq. (6) and also listed in table 1:

$$H_{EPD} = 1854.4 \times \frac{F}{(d+d_0)^2} \quad (6)$$

Plotting F/d versus d in figure 2 (d), we determined the constants α_1 and β related to the PSR model given by equation (7), and listed them in table 1.

$$F = \alpha_1 d + \beta d^2 \quad (7)$$

We then evaluate the load-independent microhardness H_{PSR} values from the following relation and list them in table 1:

$$H_{PSR} = 1854.4 \times \frac{\alpha_1 d + \beta d^2}{d^2} \quad (8)$$

Table 1 summarizes the H_v values obtained from the models analysis discussed above compared with the experimental H_v values at the saturation/plateau region. While the other two models show a reasonable agreement with our experimental results, the PSR model shows the best match. Therefore, it is noticed that in Sm1111 compound, although T_c saturates around $x=0.12$ [6, 7], the mechanical properties keep improving as x increases up to $x=0.22$.

Table 1. Fitting parameters determined from the models discussed in the text for $\text{SmFeAsO}_{1-x}\text{F}_x$ with $x=0, 0.09, 0.12, 0.22$ and 0.3 together with the H_v values determined from the models compared with experimental H_v values at the plateau region.

x	H_v (GPa) (plateau region)	Hays and Kendall (HK)			Elastic Plastic Deformation (EPD)			Proportional Specimen Resistance (PSR)		
		$A_1 \times 10^{-4}$ ($\text{N}/\mu\text{m}^2$)	W_{HK} (N)	H_{HK} (GPa)	$A_2 \times 10^{-4}$ ($\text{N}/\mu\text{m}^2$)	d_0 (μm)	H_{EPD} (GPa)	$\alpha \times 10^{-2}$ ($\text{N}/\mu\text{m}$)	$\beta \times 10^{-4}$ ($\text{N}/\mu\text{m}^2$)	H_{PSR} (GPa)
0.0	0.1443	0.7	0.5	0.1258	0.59	34.8	0.1092	0.49	0.6	0.1472
0.09	0.3878	2.0	0.2	0.3616	1.82	8.51	0.3413	0.33	2.0	0.4106
0.12	0.6011	3.0	0.8	0.4708	145	28	0.3594	1.54	2.0	0.795
0.22	0.9179	5.0	0.3	0.8405	4.16	8.1	0.7698	0.75	4.0	0.8806
0.3	0.9313	4.0	0.6	0.7992	3.72	13.4	0.7062	1.16	4.0	0.9594

4. Conclusion

Our Vickers microhardness results on a wide doping range of the FeSC Sm1111 have showed some common features with cuprates especially the ISE. Analyzing these results according to the available models, we deduced that the PSR model showed the best match with our experimental data. We confirmed that increasing the doping level in Sm1111 improves the mechanical properties of this compound and makes it more convenient for applications.

References

- [1] Kamihara Y *et al* 2008 *J. Am. Chem. Soc.* **130** 3296.
- [2] Si Q *et al* 2016 *Nature Reviews Materials* **1** 16017.
- [3] Johnson P D *et al* 2015 *Iron-based Superconductivity* (Springer).
- [4] Scalapino D J 2012 *Rev. Mod. Phys.* **84** 1383.
- [5] Johnston D C 2010 *Adv. Phys.* **59** 803.
- [6] Fujioka M *et al* 2013 *Supercond. Sci. Technol.* **26** 085023.
- [7] Fujioka M *et al* 2013 *J. Phys. Soc. Jpn.* **82** 094707.
- [8] Fujioka M *et al* 2013 *J. Phys. Soc. Jpn.* **82** 024705.
- [9] Callister W D and Rethwisch D G 2014 *Material Science and Engineering* (Wiley).
- [10] Rahal H T *et al* 2016 *J. Supercond. Nov. Magn.* DOI 10.1007/s10948-016-3654-4.
- [11] Barakat M M *et al* 2015 *J Alloy Compd.* **652** 158.
- [12] Awad R *et al* 2014 *J. Alloy. Compd.* **610** 614.
- [13] Awad R *et al* 2014 *J. Supercond. Nov. Magn.* **27** 1757.
- [14] ElMustafa A A and Stone D S 2003 *J. Mech. Phys. Solids* **51** 357.
- [15] Hays C and Kendall E G 1973 *Metallography* **6** 275.
- [16] Weiss H J 1987 *Phys. Status Solidi (a)* **99** 491.
- [17] Bull S J *et al* 1989 *Philos. Mag. Lett.* **59** 281.
- [18] Kölemen U 2006 *J. Alloys Compd.* **425** 429.